Impaired B Cell Development and Proliferation in Absence of Phosphoinositide 3-Kinase p85α

David A. Fruman,* Scott B. Snapper, Claudine M. Yballe, Laurie Davidson, Jonathan Y. Yu, Frederick W. Alt, Lewis C. Cantley

Phosphoinositide 3-kinase (PI3K) activation has been implicated in many cellular responses, including fibroblast growth, transformation, survival, and chemotaxis. Although PI3K is activated by several agents that stimulate T and B cells, the role of PI3K in lymphocyte function is not clear. The mouse gene encoding the PI3K adapter subunit p85α and its splice variants p55α and p50α was disrupted. Most p85α-p55α-p50α$^{-/-}$ mice die within days after birth. Lymphocyte development and function was studied with the use of the RAG2-deficient blastocyst complementation system. Chimeric mice had reduced numbers of peripheral mature B cells and decreased serum immunoglobulin. The B cells that developed had diminished proliferative responses to antibody to immunoglobulin M, antibody to CD40, and lipopolysaccharide stimulation and decreased survival after incubation with interleukin-4. In contrast, T cell development and proliferation was normal. This phenotype is similar to defects observed in mice lacking the tyrosine kinase Btk.

Pharmacological and biochemical approaches have established PI3K as a critical signaling intermediate in responses to a wide variety of extracellular stimuli (*1*). However, the physiological functions of different mammalian PI3K isoforms have not been tested by gene targeting. Several classes of PI3K have been distinguished on the basis of sequence similarity and substrate selectivity (*2*). The best studied PI3Ks consist of a catalytic subunit of about 110 kD and a tightly associated adapter (or regulatory) subunit of 85, 55, or 50 kD (*2*). At least three mammalian genes encode adapter subunit isoforms (p85α, p85β, and p55γ). The mouse p85α gene also encodes two smaller splice variants termed p55α and p50α (*3*, *4*). Adapter subunits increase the thermal stability of catalytic subunits (*5*) and regulate the association of the PI3K holoenzyme with membrane-associated signaling complexes (*6*). Thus, loss of adapter function might be expected to affect catalytic function as well.

We designed a targeting construct to replace the last five exons of the p85α gene with a neomycin-resistance cassette (Fig. 1A). These exons are common to all the known splice variants, and the last exon includes the putative polyadenylation signal. The mouse embryonic stem (ES) cell line TC-1 (strain 129Sv) (*7*) was transfected with the targeting construct (*8*), and two clones were identified that contained a heterozygous gene disruption (Fig. 1B) (*9*). These clones were injected into C57BL/6 blastocysts, and highly chimeric male mice were bred with C57BL/6 females to generate germ line mice. Interbreeding of p85α-p55α-p50α$^{+/-}$ mice (129Sv × C57BL/6, F_1) revealed that, although p85α gene products are not required during fetal life, less than 5% of homozygous newborns survive beyond 7 days of age (*10*). One animal (termed α198) survived to 5 weeks of age, at which time it was killed for immune system analysis (below).

RAG2-deficient mice fail to rearrange antigen receptor genes, resulting in a complete absence of mature T or B cells. Injection of pluripotent ES cells into RAG2$^{-/-}$ blastocysts gives rise to chimeric animals in which any lymphocytes must be derived from the injected ES cells. Termed the RAG2-deficient blastocyst complementation system, this allows for the testing of gene function specifically in lymphocytes and can circumvent early lethality in cases where the gene is normally required for embryonic or perinatal development (*11*). We isolated ES cell clones with a homozygous disruption of the p85α gene (Fig. 1B) and injected them into RAG2$^{-/-}$ blastocysts. Chimeric offspring were found to have ES cell–derived lymphocytes as defined by the Ly9.1 allelic marker (*10*).

Immunoblot analysis of thymocyte lysates with a monoclonal antibody (mAb) to the NH_2-terminal region of p85α confirmed the loss of p85α protein and did not detect any truncated forms that might have been transcribed and translated from the exons that were not disrupted (Fig. 1C). p85α-specific Abs also did not immunoprecipitate any PI3K activity from lysates of mutant thymocytes (Fig. 1E). The absence of p85α, p55α, or p50α protein was confirmed by immunoblot analysis with a pan-p85 antiserum that recognizes each of the three splice variants (Fig. 1C) (*9*). The residual band at 85 kD may have resulted from cross-reaction with p85β, because a p85β-specific antiserum detected expression of this isoform in low amounts in thymocytes, purified T cells, and purified B cells (Fig. 1D, lower). Expression of p85β appeared to be up-regulated in cells lacking p85α. The pan-p85 antiserum immunoprecipitated a small but detectable amount of PI3K activity from p85α$^{-/-}$ thymocytes (7% of wild type) (Fig. 1E). Expression of the catalytic subunit p110α was reduced in lymphocytes lacking p85α (Fig. 1D, upper), consistent with the instability of the p110α protein in the absence of sufficient adapter subunit concentrations (*5*). The amount of PI3K enzymatic activity in p110α precipitates was reduced by 70% (Fig. 1E).

T and B cell development can be assessed by flow cytometric analysis of lymphocyte populations stained with Abs to various surface antigens (*12*). For thymocytes, different developmental stages can be followed by using Abs to CD4 and CD8. Staining of thymocytes with these Abs revealed that normal T cell development occurred in chimeras derived from p85α$^{+/-}$ or p85α$^{-/-}$ ES cells (*10*). The absolute numbers and ratios of mature T cell subsets in the lymph nodes of chimeric animals was comparable to wild-type mice, as was the surface density of CD4, CD8, and CD3 (*10*).

B cell development can be followed by staining with Abs to B220 (expressed on all B lineage cells), immunoglobulin M (IgM) (most pre-B and mature B cells), IgD (mature B cells only), and CD43 (immature pro-B cells only). The percentage of B220$^+$ cells in the spleens of p85α$^{-/-}$RAG2$^{-/-}$ chimeras was reduced to about one-third of the percentages in p85α$^{+/-}$RAG2$^{-/-}$ chimeras or wild-type 129Sv/J mice (Fig. 2). There was a similarly reduced percentage of B cells in the spleen of mouse α198, the germ line p85α$^{-/-}$ mutant animal that survived for 5 weeks (Fig. 2). The total number of splenic B220$^+$ cells in p85α$^{-/-}$RAG2$^{-/-}$ chimeras [4.5 (±2.3) × 10^6, mean ± SD, n = 15] was

D. A. Fruman. C. M. Yballe, J. Y. Yu, L. C. Cantley, Division of Signal Transduction, Beth Israel Deaconess Medical Center, Boston, MA 02215, and Department of Cell Biology, Harvard Medical School, Boston, MA 02115, USA. S. B. Snapper, Department of Medicine, Harvard Medical School, Boston, MA 02115; Howard Hughes Medical Institute, Children's Hospital, Boston, MA 02115; Center for Blood Research, Boston, MA 02115; and Gastrointestinal Unit (Medical Services), Massachusetts General Hospital, Boston, MA 02114, USA. L. Davidson, Howard Hughes Medical Institute, Children's Hospital, Boston, MA 02115, USA. F. W. Alt, Department of Genetics, Harvard Medical School, Boston, MA 02115; Howard Hughes Medical Institute, Children's Hospital, Boston, MA 02115; and Center for Blood Research, Boston, MA 02115, USA.

*To whom correspondence should be addressed. E-mail: dfruman@bidmc.harvard.edu

reduced by greater than 85% compared with p85α$^{+/-}$RAG2$^{-/-}$ chimeras [33.4 (±6.7) × 10^6, $n = 3$, $P < 0.01$] and wild-type mice [30.3 (±15.7) × 10^6, $n = 12$, $P < 0.0001$]. Splenic T cell numbers were not significantly different. The B220$^+$ population in the spleens of p85α$^{-/-}$RAG2$^{-/-}$ chimeras and of mouse α198 consisted mainly of cells with a high surface density of IgM (Fig. 2), which is characteristic of newly emerging B cells, and there was a corresponding reduction in the frequency of IgD^{hi} IgM^{lo} cells (*10*). There were similar B cell deficits in lymph nodes from p85α$^{-/-}$RAG2$^{-/-}$ chimeras. Analysis of bone marrow cells showed that p85α$^{-/-}$RAG2$^{-/-}$ chimeras and mouse α198 had a relative increase in the pro-B (CD43^{lo}B220$^+$) subpopulation relative to the CD43$^-$ pre-B and mature B cell subpopulation (Fig. 2). These results are consistent with a role for p85α in progression from pro-B to mature B cells. Finally, p85α$^{-/-}$RAG2$^{-/-}$ chimeras showed a nearly complete absence of the CD5$^+$ subset of peritoneal B cells (Fig. 2).

Bruton's tyrosine kinase (Btk), a B cell–specific member of the Tec kinase family, is a putative downstream effector of PI3K in B cells (*13*). Activation of Btk involves recruitment to the membrane through an interaction between PI3K lipid products and the pleckstrin homology (PH) domain of Btk (*14*). Mutations in human Btk are the cause of the immunodeficiency X-linked agammaglobulinemia, which is associated with severe reductions in mature B cells and in serum immunoglobulin (*15, 16*). In mice, Btk mutations cause a more mild immunodeficiency resulting from moderate reductions in mature B cells, impaired expansion of B cell precursors, and inability to respond to certain B cell activators in vitro and in vivo (*17, 18*). The p85α$^{-/-}$RAG2$^{-/-}$ chimeras had similar B cell abnormalities. B cell development was examined in CBA/N.*Xid* mice with a mutated PH domain of Btk. In agreement with previous findings (*18*), *xid* mice had moderately

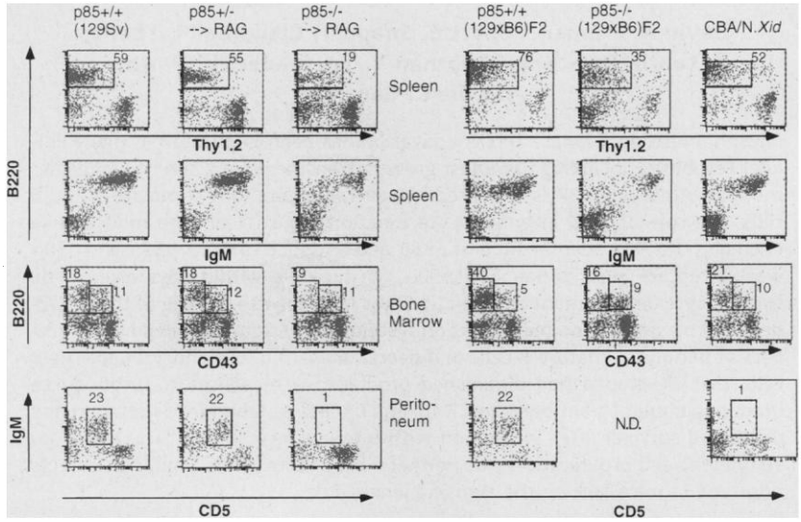

Fig. 2. B cell development is impaired in the absence of p85α-p55α-p50α. For each row of histograms, the first three boxes depict a representative flow cytometric experiment comparing chimeric animals with an age-matched wild-type 129Sv/J mouse. The second set of three boxes depicts an experiment in which a germ line p85α$^{-/-}$ animal (α198) was compared with a wild-type littermate and with a CBA/N.*Xid* mouse. The staining Abs are indicated adjacent to the axes. The numbers indicate the percentage of cells contained within the rectangular regions shown. Similar results were observed in 15 p85α$^{-/-}$RAG$^{-/-}$ chimeras, 5 *xid* mice, and 3 p85α$^{+/-}$/RAG$^{-/-}$ chimeras. N.D., not determined.

Fig. 1. Targeted disruption of the mouse p85α gene. (**A**) Diagram of the targeting construct and probes (labeled 1, 2, and 3) used for detecting homologous recombination. Black boxes denote exons. (**B**) Southern blot of Bam HI–digested genomic DNA with probe 1. The designation 75.0 is a subclone of heterozygous ES cell line 75 that was identified with a probe external to the regions of homology (probe 3). Subclones 75.2 and 75.7 are homozygous mutant ES cell lines. (**C**) Immunoblots demonstrating loss of p85α-p55α-p50α expression in thymocytes derived from homozygous mutant ES cells. Left panel, anti-p85α mAb; right panel, anti–(pan)-p85 antiserum. Thymocytes were prepared from wild-type (129Sv) mice (denoted +/+), p85α$^{+/-}$/RAG$^{-/-}$ chimeras (+/−), and two different p85α$^{-/-}$RAG$^{-/-}$ chimeras (−/−). A 100-μg sample of protein was loaded per lane. (**D**) Immunodetection of p110α and p85β in 3 × 10^6 thymocytes, purified T cells, or purified B cells of wild-type (129Sv) mice (+/+), p85α$^{-/-}$RAG$^{-/-}$ chimeras (−/−), or from 0.5 × 10^6 fibroblasts derived from wild-type (WT), p85α$^{-/-}$ (α−), or p85β$^{-/-}$ (β−) embryos (129Sv × C57Bl/6, F_2). The production of embryonic fibroblast lines and the generation of p85β-deficient mice will be described elsewhere. These results are representative of two experiments. (**E**) Reduced PI3K enzymatic activity in cells lacking p85α gene products. Samples (500 μg) of protein from thymocyte lysates of wild-type (129Sv) mice (+/+) or p85α$^{-/-}$RAG$^{-/-}$ chimeras (−/−) were immunoprecipitated with the indicated antibodies, and immune complex kinase assays were performed with a substrate mixture of phosphatidylinositol (PtdIns), PtdIns-4-phosphate, and PtdIns-4,5-bisphosphate as described (*26*). The products were separated by thin-layer chromatography and radioactivity quantitated with a Molecular Imager (Bio-Rad). The numbers indicate the radioactivity in the PtdIns-3,4,5-trisphosphate spot after subtraction of the radioactivity in a nonimmune control precipitate, expressed as arbitrary phosphorimager units. Results are representative of two experiments.

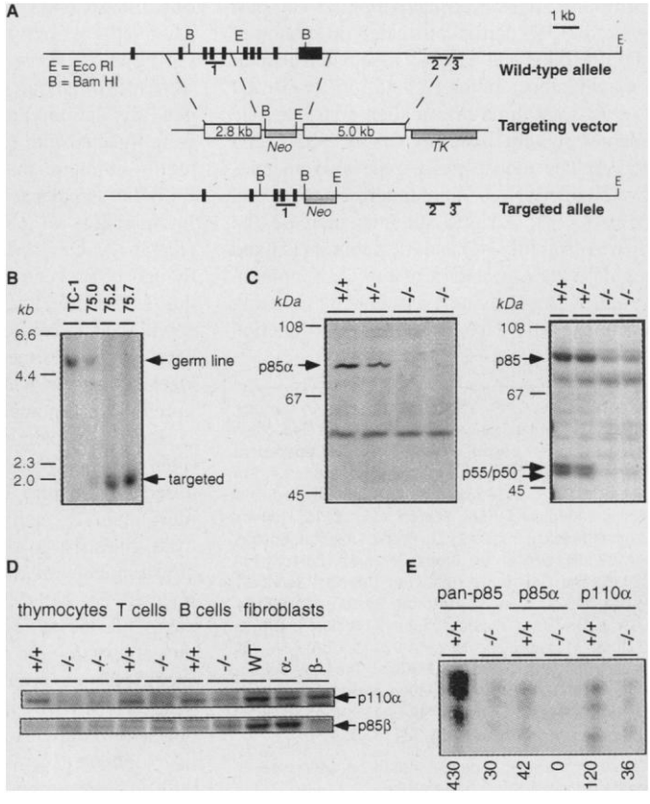

reduced frequencies of B cells in the spleen [8.6 ($\pm$4.0) $\times$ 10^6, $n = 4$, $P < 0.001$ compared with wild type], a shift toward IgM^{hi} cells, and an absence of $CD5^+$ B cells in the peritoneum (Fig. 2).

Serum Ig concentrations were measured by isotype-specific enzyme-linked immunosorbent assay (ELISA) (*19*). The mean concentrations of IgM, IgG2a, IgG3, and IgA were decreased by 92, 89, 97, and 89%, respectively, in serum from $p85\alpha^{-/-}$ $RAG2^{-/-}$ chimeras relative to wild-type 129Sv mice (Fig. 3). The amount of serum IgG1 in the $p85\alpha^{-/-}RAG2^{-/-}$ chimeras was reduced by less than 50%. As reported previously (*18*), *xid* mice had reduced concentrations of all isotypes. Thus, mice whose B cells lack either functional Btk or p85α exhibit reductions in serum Ig levels. All Ig isotype concentrations in serum from $p85\alpha^{+/-}$ $RAG2^{-/-}$ chimeras were comparable with wild type.

Lymphocyte function was assessed by measuring [^{3}H]thymidine incorporation of purified B or T cells stimulated with various agonists (*20*). The p85α-p55α-p50α–deficient B cells had reproducible defects in proliferative responses to the polyclonal B cell activators anti-IgM, lipopolysaccharide (LPS), and anti-CD40 (Fig. 4A). The anti-IgM response was barely above background levels and was only weakly enhanced by addition of recombinant murine interleukin-4 (IL-4). Failure to respond to anti-IgM was not due to reduced surface expression of IgM (Fig. 2). The LPS response averaged 6% of wild type and was partially restored by IL-4. Interestingly, although knockout B cells responded poorly to anti-CD40 alone (12% of wild type), treatment with anti-CD40 plus IL-4 triggered thymidine incorporation to a similar extent as in wild-type cells (Fig. 4A), indicating that p85α-p55α-p50α–deficient B cells do not have an absolute defect in cell cycle entry. B cells from $p85\alpha^{+/-}RAG^{-/-}$ chimeras responded normally to all agonists (*10*). Pretreatment of wild-type B cells with the PI3K inhibitor Ly294002 inhibited proliferation to a similar extent as loss of p85α-p55α-p50α for all agonists tested (Fig. 4A), suggesting that the loss of either adapter expression or catalytic function produces a similar outcome. These findings imply that other PI3K adapter subunits do not have redundant functions in B cells. The pattern of proliferative defects was very similar to the defects observed in *xid* B cells (*18*) (Fig. 4A), although *xid* B cells responded considerably better to the high concentration of LPS (10 μg/ml) used in these experiments.

T cells without p85α gene products were not deficient in proliferative responses to antigen receptor (anti-CD3) stimulation in the absence or presence of costimulation (anti-CD28) or cytokines (IL-2) (Fig. 4B). To determine if PI3K catalytic function was required for responses to anti-CD3, we treated wild-type T cells with Ly294002 before stimulation. Inhibition of PI3K strongly reduced responses to anti-CD3 alone or to anti-CD3 plus IL-2 (Fig. 4B). Together these data suggest that activation of PI3K is an essential step in CD3- and CD3-IL-2–mediated signaling pathways, but that the remaining adapter isoforms and residual PI3K catalytic activity in p85α-p55α-p50α–deficient cells are suffi-

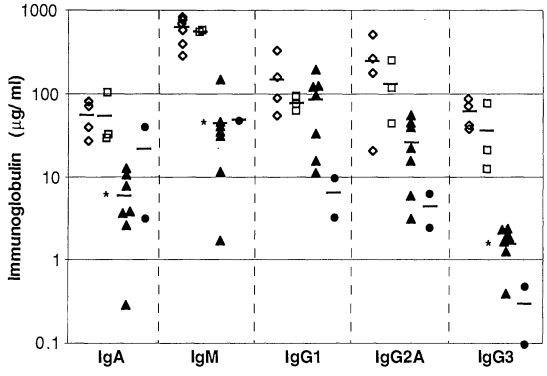

Fig. 3. Serum Ig concentrations are reduced in $p85\alpha^{-/-}RAG2^{-/-}$ chimeras and *xid* mice. Concentrations of different Ig isotypes were determined by ELISA and plotted on a semi-logarithmic graph. Symbols: open diamonds, $p85\alpha^{+/+}$ (129Sv/J); open squares, $p85\alpha^{+/-}RAG2^{-/-}$; closed triangles, $p85\alpha^{-/-}/RAG2^{-/-}$; closed circles, CBA/N.*Xid*. Mean values are indicated by bold hashmarks. Statistical analysis was done (Student's *t* test) to determine whether Ig concentrations from chimeric mice were significantly different than from wild-type mice. *$P < 0.05$.

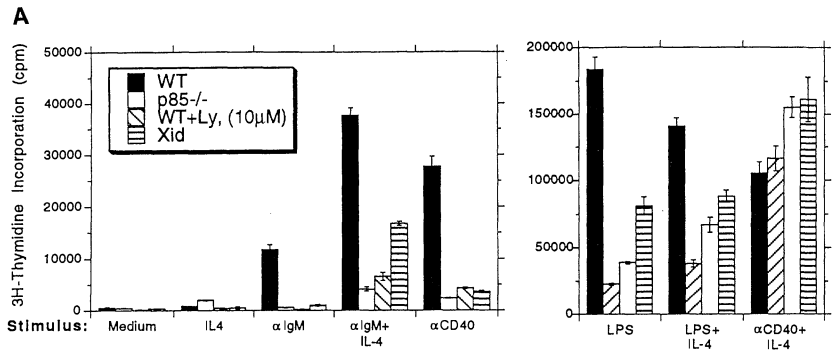

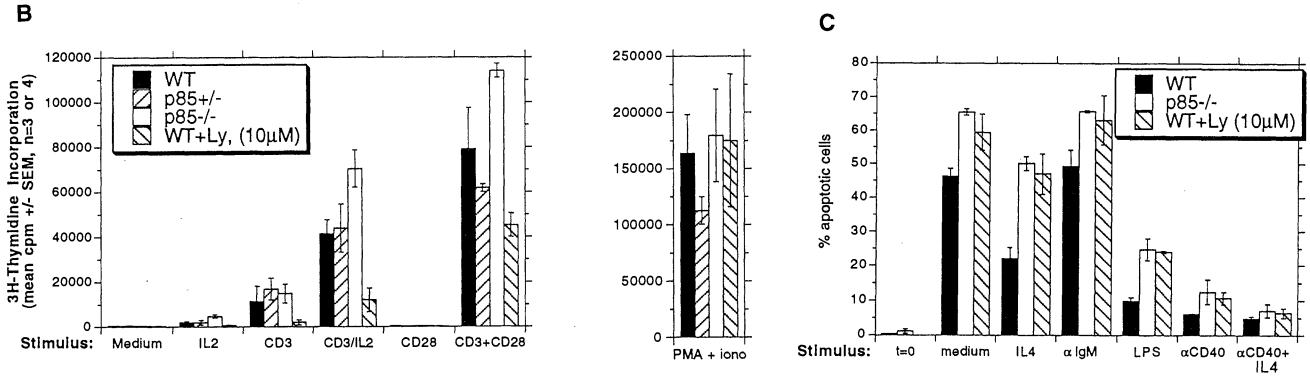

Fig. 4. Role of p85α-p55α-p50α in proliferation and survival. (**A**) B cell proliferation data are expressed as mean counts per minute ($\pm$ SEM) of triplicates from a single thymidine incorporation assay (α, antibody; Ly, Ly294002). Results are representative of three to six experiments. (**B**) T cell proliferation data are expressed as the mean counts per minute ($\pm$ SEM) of three or four separate experiments. PMA plus ionomycin (iono) is a stimulus that bypasses membrane signaling events. (**C**) $B220^+$ cells undergoing apoptosis were identified by flow cytometric analysis of DNA content. Apoptosis is expressed as the percentage of cells with a DNA content of less than 2N, mean $\pm$ range, $n = 2$.

cient to transmit the signal. The presence of equivalent amounts of p85β in T cells and B cells (Fig. 1D) suggests that the differences observed in T and B cell function cannot be explained by differential expression of this adapter isoform. Treatment with Ly294002 only slightly inhibited the proliferative response to costimulation with anti-CD3 plus anti-CD28 (Fig. 4B). Although the p85p110-type PI3K associates with CD28, its function in CD28-driven proliferation is controversial (*21*); our results are consistent with studies showing that PI3K inhibitors do not block CD28-mediated costimulation of resting mouse T cells (*22*).

We further investigated B cells for cell cycle distribution and apoptosis using flow cytometric analysis (*23*). The percentage of cells in the S and G_2-M phases of the cell cycle correlated with the thymidine incorporation measurements (*10*). Apoptotic cells were quantitated by gating on B cells with sub-G_1 DNA content (Fig. 4C). After 36 hours in medium alone, there was an increased percentage of apoptotic B cells from p85α$^{-/-}$RAG$^{-/-}$ chimeras and from wild-type cells treated with Ly294002 compared with untreated wild-type cells. The apparent role for p85α-p55α-p50α–associated PI3K activity in survival of resting B cells may explain the decreased numbers of B cells observed in peripheral lymphoid organs (Fig. 2). Under all conditions where drug-treated or knockout B cells showed deficient proliferation, an increase in the percentage of apoptotic cells was observed. However, none of the agonists increased cell death above the level observed in medium alone, and only IL-4 alone appeared to provide a specific survival advantage to wild-type cells. Together these data suggest that PI3K is critical for serum- and IL-4–mediated survival and for agonist-induced cell cycle entry, but it is dispensable for survival signals induced by LPS or anti-CD40. Of note, anti-IgM treatment stimulated proliferation in wild-type cells (Fig. 4A) but did not change the extent of apoptosis, whereas IL-4 alone, which did not induce significant proliferation, provided a potent survival signal (Fig. 4C). These observations support the notion that cell survival and entrance into the cell cycle are not necessarily linked. In agreement with previous reports (*24*), we observed greater apoptosis in *xid* B cells after culture in medium alone, and *xid* B cells showed a similar extent of death as p85α-p55α-p50α–deficient B cells after agonist treatment (*10*).

We have presented genetic evidence for a critical function of PI3K p85α gene products in B cell development, proliferation, and survival. This phenotype is not merely the result of poor chimerism in the reconstituted RAG-deficient mice, because nonchimeric p85α$^{-/-}$ mutant mouse α198 exhibited a phenotype indistinguishable from the chimeras. In addition, a separate group has disrupted the p85α gene and observed a similar phenotype (*25*). The observation of similar B cell deficits in p85α- and Btk-deficient mice strengthens the model that PI3K and Btk are components of a common signaling pathway. The adapter isoforms encoded by the p85α gene appear to be critical for PI3K catalytic function, as p85α-deficient cells have greatly reduced p110α expression and activity, and similar B cell proliferation defects are observed in wild-type cells treated with a PI3K inhibitor. Finally, our results demonstrate that PI3K plays separable roles in B cell survival and proliferation.

References and Notes

1. A. Toker and L. C. Cantley, *Nature* **387**, 673 (1997); B. Vanhaesbroeck, S. J. Leevers, G. Panayotou, M. D. Waterfield, *Trends in Biochem. Sci.* **22**, 267 (1997).
2. J. Domin and M. D. Waterfield, *FEBS Lett.* **410**, 91 (1997).
3. D. A. Fruman, L. C. Cantley, C. L. Carpenter, *Genomics* **37**, 113 (1996).
4. K. Inukai *et al.*, *J. Biol. Chem.* **271**, 5317 (1996); D. A. Antonetti, P. Algenstaedt, C. R. Kahn, *Mol. Cell. Biol.* **16**, 2195 (1996).
5. J. Yu *et al.*, *Mol. Cell. Biol.* **18**, 1379 (1998).
6. B. C. Duckworth and L. C. Cantley, in *Handbook of Lipid Research: Lipid Second Messengers*, R. M. Bell and J. H. Exton, Eds. (Plenum, New York, 1996), vol. 8, pp. 125–175.
7. C. Deng, A. Wynshaw-Boris, F. Zhou, A. Kuo, P. Leder, *Cell* **84**, 911 (1996).
8. A 4.5-kb genomic fragment encompassing exons 11 through 15 of the mouse p85α gene (*3*) was replaced by a 2-kb pgk-*neo* cassette. TC-1 ES cells (2×10^7) were electroporated with 20 μg of linearized DNA and subjected to positive selection with G418 (0.4 mg/ml) and negative selection with gancyclovir (1 μM). Two clones (designated 75 and 134) containing heterozygous disruptions of the gene were identified by Southern (DNA) blot analysis with probes flanking the 3′ homology region and with probes internal to both the 5′ and 3′ homology regions. The presence of a single integration event was verified by hybridization with a Neo probe (*10*). Germ line transmission was obtained with clone 75. For genotyping of mice, we subjected tail DNA to polymerase chain reaction analysis using two primer sets in the same reaction, one set (5′-TCCAAATGAAAAGAACGGCTATC-3′ and 5′-TGTACCAAAGTCACTGAAAAATCTGTT-3′) detecting the endogenous allele, and the other set (5′-AAGATAATATTGAAGCTGTAGGGAAAAA-3′ and 5′-TGTTAAGAAGGGTGAGAACAGAGTACC-3′) detecting a DNA segment in the targeted allele. Homozygous mutant cell lines were isolated by selecting heterozygous cells (clone 75) in increased concentrations of G418 (4.8 mg/ml). These lines and the parental clone 75 were subcloned before injection into RAG2-deficient blastocysts as described (*11*). Animal experiments were carried out in accordance with institutional guidelines.
9. Southern blots were prepared with ZetaProbe GT membranes (Bio-Rad) and hybridized with ^{32}P-labeled DNA probes. Protein immunoblots were prepared with nitrocellulose membranes (Bio-Rad), probed with polyclonal or monoclonal antibodies, and developed with enhanced chemilumiscence reagents (NEN). Monoclonal antibody to p85α (anti-p85α) and polyclonal anti–pan-p85 were purchased from Upstate Biotechnology, Inc., polyclonal anti-p110α from Santa Cruz, and polyclonal anti-p85β was generated by immunizing rabbits with a keyhole limpet hemacyanin (KLH)–conjugated peptide derived from mouse p85β, TyrProPheArgArgGluArgProGluAspLeuGluLeu. Immunoprecipitations were performed with the same antibodies, except that the monoclonal anti-p85α was mixed with a second monoclonal anti-p85α from Transduction Laboratories, and the anti-p110α was a gift of K. Auger.
10. D. A. Fruman, unpublished results.
11. J. Chen, R. Lansford, V. Stewart, F. Young, F. W. Alt, *Proc. Natl. Acad. Sci. U.S.A.* **90**, 4528 (1993).
12. Single-cell suspensions were prepared from lymphoid organs and red blood cells lysed in hypotonic buffer. Cells were stained with fluorescein isothiocyanate (FITC)–, phycoerythrin- and CyChrome-labeled antibodies (Pharmingen and Southern Biotech) and analyzed on a FACScalibur with CellQuest software (Becton-Dickinson) with the use of a live cell gate.
13. A. M. Scharenberg *et al.*, *EMBO J.* **17**, 1961 (1998).
14. K. Salim *et al.*, *ibid.* **15**, 6241 (1996); L. E. Rameh *et al.*, *J. Biol. Chem.* **272**, 22059 (1997); S. Bolland, R. N. Pearse, T. Kurosaki, J. V. Ravetch, *Immunity* **8**, 509 (1998).
15. S. Tsukada *et al.*, *Cell* **72**, 279 (1993).
16. D. Vetrie *et al.*, *Nature* **361**, 226 (1993).
17. J. D. Thomas *et al.*, *Science* **261**, 355 (1993); D. J. Rawlings *et al.*, *ibid.*, p. 358; J. D. Kerner *et al.*, *Immunity* **3**, 301 (1995).
18. W. N. Khan *et al.*, *Immunity* **3**, 283 (1995).
19. We measured Ig's in serial dilutions of serum using microtiter plates (Dynatech) and antibody pairs specific for different mouse Ig isotypes (Pharmingen). *P*-Nitrophenylphosphate was used as a substrate for the alkaline phosphatase–conjugated secondary antibodies, and the absorbance at 405 nm was measured in a microplate reader (Molecular Devices).
20. T cells were purified from lymph node by negative selection with anti–class II magnetic beads (Miltenyi Biotech), yielding greater than 90% T lymphocytes (Thy1$^+$). B cells were purified from spleen and lymph node by negative selection with a combination of magnetic beads specific for CD43, CD11b, and CD11c (Miltenyi), yielding greater than 95% B lymphocytes (B220$^+$), except in the case of p85α-deficient cells, which were 60 to 85% pure. T or B cells (5×10^4) were cultured in triplicate in 96-well dishes (Falcon) in a total volume of 100 μl of medium [RPMI containing 10% heat-inactivated fetal calf serum (FCS), 10 mM Hepes, pH 7.4, penicillin (100 units/ml), streptomycin (100 μg/ml), 2 mM L-glutamine, and 50 μM 2-mercaptoethanol]. For plate-bound antibody stimulation, plates were precoated with anti-CD3ε (Pharmingen) at various concentrations or anti-CD28 (Pharmingen) at 10 μg/ml (or both) in 1× phosphate-buffered saline (PBS) for 1.5 hours at 37°C and washed in 1× PBS containing 5% FCS before cell addition. Soluble agonists were included at the following final concentrations: phorbol 12-myristate 13-acetate (PMA) (20 ng/ml , Calbiochem), ionomycin (1 μM, Calbiochem), anti-IgM [F(ab′)$_2$, 10 μg/ml, Jackson ImmunoResearch], LPS (10 μg/ml, Sigma), anti-CD40 (1 μg/ml, Pharmingen), recombinant murine IL-2 (100 U/ml, Genzyme), and IL-4 (2 ng/ml, Pharmingen). Approximately 5×10^4 cells in 50 μl were added to wells containing 50 μl of agonists at 2× final concentration. Where indicated, cells were pretreated for 15 min at 37°C with 10 μM Ly294002 (Calbiochem) before they were added to wells. Forty-eight hours later, 50 μl of medium containing [^{3}H]thymidine (20 μCi/ml, NEN) was added to each well. Cells were harvested 12 hours later with a TomTec plate harvester and counted in a BetaPlate scintillation counter (Wallac).
21. J. E. Hutchcroft and B. E. Bierer, *J. Immunol.* **156**, 4071 (1996); S. G. Ward, *Biochem. J.* **318**, 361 (1996).
22. K. E. Truitt *et al.*, *J. Immunol.* **155**, 4702 (1995).
23. Purified B cells (1.5×10^5) were cultured for 36 hours in 48-well dishes under conditions identical to the thymidine incorporation assays. Cells were then harvested, stained with anti-B220–FITC, fixed in 50% ice-cold ethanol, treated with ribonuclease, and stained with propidium iodide. Aggregates and B220$^-$ cells were excluded, and the percentage of cells with sub-G1 DNA content was quantitated with CellQuest software. Similar results were observed when apoptosis was measured after 18 hours (*10*).
24. R. T. Woodland, M. R. Schmidt, S. J. Korsmeyer, K. A. Gravel, *J. Immunol.* **156**, 2143 (1996); J. S. Anderson, M. Teutsch, Z. Dong, H. H. Wortis, *Proc. Natl. Acad. Sci. U.S.A.* **93**, 10966 (1996).
25. H. Suzuki *et al.*, *Science* **283**, 390 (1999).

26. C. L. Carpenter *et al.*, *J. Biol. Chem.* **265**, 19704 (1990).

27. We thank B. Sleckman, S. Thomas, G. Rathbun, and C. Carpenter for suggestions, K. Auger for anti-p110α, J. Lawitts for blastocyst injections, D. Pollard for mouse husbandry and genotyping, D. Kim for help with fibroblast culture, and K. Lee-Fruman for a critical reading of the manuscript. Supported by grants from NIH (to L.C.C., F.W.A., and S.B.S.), a fellowship from the Damon Runyon–Walter Winchell Cancer Research Fund (to D.A.F.), the Leukemia Society of America (to D.A.F.), and the Howard Hughes Medical Institute (to F.W.A.).

6 August 1998; accepted 17 December 1998

Role of Serotonin in the Paradoxical Calming Effect of Psychostimulants on Hyperactivity

Raul R. Gainetdinov, William C. Wetsel, Sara R. Jones, Edward D. Levin, Mohamed Jaber,* Marc G. Caron†

The mechanism by which psychostimulants act as calming agents in humans with attention-deficit hyperactivity disorder (ADHD) or hyperkinetic disorder is currently unknown. Mice lacking the gene encoding the plasma membrane dopamine transporter (DAT) have elevated dopaminergic tone and are hyperactive. This activity was exacerbated by exposure to a novel environment. Additionally, these mice were impaired in spatial cognitive function, and they showed a decrease in locomotion in response to psychostimulants. This paradoxical calming effect of psychostimulants depended on serotonergic neurotransmission. The parallels between the DAT knockout mice and individuals with ADHD suggest that common mechanisms may underlie some of their behaviors and responses to psychostimulants.

The catecholamine dopamine (DA) is present in both the central and peripheral nervous systems, where it controls a variety of different physiological processes (*1*). Perhaps one of the most important regulators of dopaminergic function is the DA transporter (DAT) (*2*). This transporter is located on the plasma membrane of DA neurons, where it controls the concentrations of DA by rapidly removing the transmitter from the extracellular space and localizing it into the cytoplasm (*3*). A long-term interest in this transporter derives from its role as an endogenous target for psychostimulants, antidepressants, and several neurotoxins (*3*). Disruption of the DAT gene in mice (*4*) results in a phenotype that includes behavioral abnormalities, neuroendocrine dysfunction, dwarfism, and altered sensitivities to certain drugs (*2*, *5*). A prominent characteristic of these mice is their marked hyperactivity (*4*). This hyperkinetic behavior is consistent with the loss of transporter function and the resultant high concentrations of extracellular DA in the striata of these mice (*2*).

Recently, an association between polymorphisms in the noncoding regions of the human DAT and ADHD has been suggested (*6*). ADHD is a condition that is manifested by impulsivity, hyperactivity, and inattention (*7*). These symptoms are also defined as hyperkinetic disorder (HKD) (*8*). It is estimated that 3 to 6% of school-aged children are affected by this condition (*9*). Since the 1930s, treatment has involved the use of psychostimulant compounds that paradoxically serve to attenuate the hyperactivity and often improve cognitive performance (*9*, *10*). Although psychostimulants preferentially inhibit the DAT, they also block the action of other monoamine transporters (*3*, *5*, *11*). As a result, extracellular concentrations of DA, norepinephrine (NE), and serotonin (5-HT) can be elevated. Although dysregulation of each of these monoamine systems has been postulated to be involved in ADHD-HKD, it is commonly believed that the DA system is preferentially implicated in the etiology and pharmacotherapy of these disorders (*9*, *12*).

Drugs that block the DAT result in a pronounced increase in extracellular DA in brain regions that mediate enhanced locomotion and stereotypic behavior (*2–4*, *11*). DAT knockout (KO) mice were placed into a novel environment, and locomotor, rearing, and stereotypic activities were monitored (*13*). DAT-KO animals exhibited substantially higher levels of activity than wild-type mice (Fig. 1, A to C). Whereas the DAT-KO mice showed minimal habituation to the novel environment over 240 min of observation, habituation occurred within the first 30 to 40 min for the wild-type animals. Hyperactivity in the DAT-KO animals appeared to be novelty driven because locomotor activity was about 12-fold higher in the novel environment (Fig. 1D). Moreover, repetitive exposure to the open field augmented the activity of the DAT-KO mice over seven consecutive days of testing, whereas locomotor responses of the wild-type mice showed habituation (*14*). These results suggest that the DAT-KO animals might be less able to adapt to novel stimuli than the wild-type controls.

Extracellular DA concentrations were sampled by microdialysis in freely moving mice in both the familiar and novel environments (*15*). Despite the fact that DAT-KO mice have fivefold higher concentrations of extracellular DA (*2*), no differences were discerned as a function of time when samples were taken from mice in either environment (Fig. 1E). Dopaminergic neurotransmission, however, was required for the presence of locomotor activity because haloperidol, a DA receptor antagonist, suppressed activity in both the wild-type (*14*) and DAT-KO mice (Fig. 1F). These data suggest that although the enhanced spontaneous locomotor activity in the DAT-deficient animals was not due to additional augmentation of dopaminergic neurotransmission in striatum, it was dependent on dopaminergic tone (see also Fig. 4C). These findings indicate that additional mechanisms may be responsible for the novelty-induced hyperactivity of the DAT-KO mice.

An aspect of ADHD-HKD that may accompany or occur independently of the hyperactivity involves cognition. Animals were tested in an eight-arm radial maze with a win-shift paradigm over 21 consecutive days (*16*). In this procedure, only the first entry in each arm was rewarded. Initially, performance was very poor for both genotypes (Fig. 2A). As training progressed, wild-type mice attained high levels of performance within the first several sessions. As a group, the DAT-KO mice were significantly impaired. These differences in performance did not appear to be due to possible motivational differences because animals from both groups consumed practically identical amounts of food in the maze (*17*).

Another manner of evaluating performance in the radial maze is to examine the response patterns that are made while acquiring the task. One type of response is that of perseveration (*18*). DAT-KO mice made significantly more

R. R. Gainetdinov, S. R. Jones, M. Jaber, M. G. Caron, Howard Hughes Medical Institute Laboratories, Departments of Cell Biology and Medicine, Duke University Medical Center, Durham, NC 27710, USA. W. C. Wetsel, Departments of Psychiatry and Medicine (Endocrinology), Duke University Medical Center, Durham, NC 27710, USA. E. D. Levin, Department of Psychiatry, Duke University Medical Center, Durham, NC 27710, USA.

*Present address: CNRS UMR5541, University of Bordeaux II Victor Segalen, 146 Rue Leo Saignat, 33076 Bordeaux Cedex, France.

†To whom correspondence should be addressed. E-mail: caron002@mc.duke.edu